PHYSICAL REVIEW A VOLUME 46, NUMBER 9 1 NOVEMBER 1992

One-atom lasers

Yi Mu and C. M. Savage
Department of Physics and Theoretical Physics, Australian National University, Canberra, Australian Capital Territory 2601, Australia
(Received 16 March 1992; revised manuscript received 2 June 1992)

One-atom lasers are important because their governing equations can be solved exactly, even with a quantized field. We present a fully quantum-mechanical treatment of one-atom lasers modeled by quantum-optical master equations. These are solved numerically without any significant approximations. We show that laser action is possible with one atom, and that it might be achievable experimentally. Laser action is characterized by the dominance of stimulated emission over spontaneous emission. We use the one-atom laser model to investigate, without approximation, some interesting generic laser phenomena. Under certain conditions lasers produce intensity squeezed light, and then the laser linewidth increases with the pumping rate, in contrast with standard lasers. We also report "self-quenching" behavior: lasers with incoherent pumping out of the lower laser level turn off when the pumping is sufficiently fast because the coherence between the laser levels is destroyed.

PACS number(s): 42.55.−f, 42.50.Dv

I. INTRODUCTION

Treatments of the laser in which the light field, as well as the atoms, is quantized are usually based on approximations that make the mathematical problems manageable. An important such approximation is that the number of lasing atoms N_a is large enough that some quasiprobability distribution for the laser satisfies a Fokker-Planck equation [1]. This paper investigates lasers that have only one or two lasing atoms and so do not allow this approximation. Such lasers are potentially realizable in the small, high finesse optical cavities currently used in optical cavity QED experiments [2].

Since one-atom lasers may operate with only a small number of photons in the laser cavity (perhaps less than ten) the semiclassical approximation is not reliable and a fully quantum-mechanical treatment, including quantization of the field, must be used. We show that it is reasonable to use the term "laser" since the light is dominantly produced by stimulated emission. We then use our one-atom laser model to investigate phenomena that are not restricted to one-atom lasers: laser squeezing and associated linewidth broadening with increased pump rate. Finally we consider "self-quenching," which may be particularly relevant to one-atom lasers.

In this paper we numerically solve master equations for three- and four-level one and two-atom lasers. Provided the basis set of states for the field is sufficiently large, no approximations beyond those already in the master equation are involved in the numerical solution. In principle, we can study any laser property this way.

Smith and Gardiner have previously modeled lasers with arbitrary numbers of atoms [3], however, in order to control numerical instabilities they made the assumption that a reservoir level was present [4]. This assumption excludes interesting phenomena such as laser squeezing [5–8].

The paper is organized as follows. Section II presents the master equations for the particular laser models we investigate: incoherently pumped two- and three-level lasers, and a coherently or incoherently pumped four-level laser. The method of numerical solution of the master equations is described. Section III investigates the conditions under which one atom in a cavity is really a laser and estimates the requirements for its construction. In Sec. IV we consider the photon statistics of the laser light. Recent predictions of intensity squeezed light generation by conventionally pumped lasers are confirmed [5–8]. This is significant since, unlike previous work, our solutions involve no approximations. Unlike conventional lasers the linewidth of "squeezed lasers" can increase with the pumping rate. In Sec. V we investigate a novel phenomenon in incoherently pumped lasers: the lasing turns off for sufficiently high pump rates. We call this self-quenching. It occurs when the coherence between the lasing levels is damped by the incoherent pumping.

II. MODEL

The systems under investigation consist of a two-, three-, or four-level atom coupled to a single mode of an optical cavity, Fig. 1. The atomic levels are described by the atomic lowering and raising operators $\sigma_{ij}^{-}=|i\rangle\langle j|$ and $\sigma_{ij}^{+}=|j\rangle\langle i|$, obeying the standard anticommutation relations. The cavity mode is assumed to be resonant with the atomic lasing transition and is described by the boson annihilation and creation operators a and $a^{\dagger}$. The laser transition interacts with the cavity mode via the electric dipole, rotating-wave approximation, Jaynes-Cummings Hamiltonian

$$H_{\mathrm{JC}}=i\hbar g(a^{\dagger}\sigma_{kl}^{-}-a\sigma_{kl}^{+}) , \tag{1}$$

where the lasing occurs between levels k and l, and g is the atom-cavity coupling strength

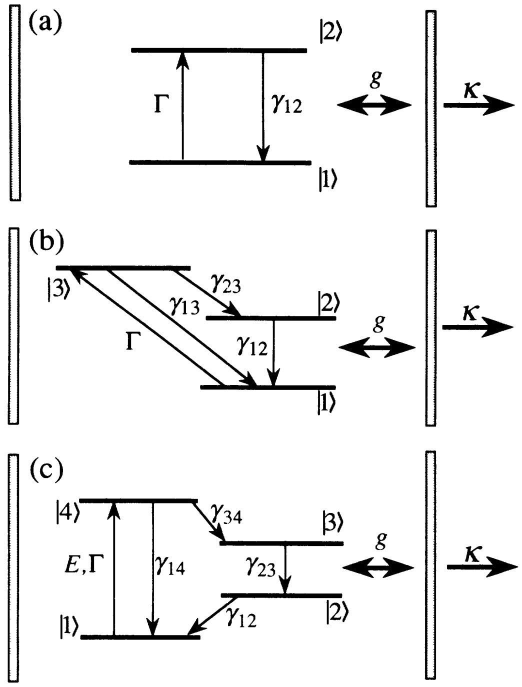

FIG. 1. Schematic diagrams of the laser systems considered in this paper. Pumping is either incoherent at rate Γ or coherent with field strength proportional to E. The arrow labels correspond to terms in the master equation (4). The shaded vertical bars represent cavity mirrors. (a) Two-level laser; (b) three-level laser; (c) four-level laser.

$$g=\left[\frac{3\pi\gamma_L c^3}{2\omega^2}\right]^{1/2}|u(\mathbf{r})| \ , \tag{2}$$

where γ_L is the decay rate between the laser levels, ω is the laser transition frequency, and $u(\mathbf{r})$ is the cavity mode function.

In the interaction picture, rotating at the driving field frequency, coherent pumping of the atom is represented by

$$H_E=i\hbar E(\sigma_{1\mu}^{-}-\sigma_{1\mu}^{+}) \ , \tag{3}$$

where E is proportional to the pump field strength. The upper pump level label μ depends on the model used, and is 2 for the two-level atom, 3 for the three-level atom, and 4 for the four-level atom. Alternatively the atoms may be pumped incoherently at the rate Γ.

Following standard techniques, the atom and cavity mode may be coupled to suitable reservoirs and Markoffian master equations for the reduced density operator ρ derived [1,9]. The cavity mode is damped by losses through the cavity mirrors at the rate 2κ photons per second. Atomic spontaneous emission out the side of the cavity, from level i to level j, occurs at the rate γ_{ij}. Only those γ_{ij} shown in Fig. 1 are assumed to be nonzero in our numerical calculations. The resulting interaction picture master equation is then

$$\begin{aligned}\frac{\partial\rho}{\partial t}&=\frac{1}{i\hbar}[H_E+H_{\mathrm{JC}},\rho]+L_C\rho+L_P\rho+\sum_{\substack{i,j=1\\(i\neq j,i<j)}}^{\mu}L_{Aij}\rho \ ,\\ L_C\rho&=\kappa(2a\rho a^\dagger-a^\dagger a\rho-\rho a^\dagger a) \ ,\\ L_{Aij}\rho&=\frac{\gamma_{ij}}{2}(2\sigma_{ij}^{-}\rho\sigma_{ij}^{+}-\sigma_{ij}^{+}\sigma_{ij}^{-}\rho-\rho\sigma_{ij}^{+}\sigma_{ij}^{-}) \ ,\\ L_P\rho&=\frac{\Gamma}{2}(2\sigma_{1\mu}^{+}\rho\sigma_{1\mu}^{-}-\sigma_{1\mu}^{-}\sigma_{1\mu}^{+}\rho-\rho\sigma_{1\mu}^{-}\sigma_{1\mu}^{+}) \ .\end{aligned} \tag{4}$$

Incoherent pumping at rate Γ from level $|1\rangle$ to level $|\mu\rangle$ is modeled as the inverse process to spontaneous emission [1]. The generalization to more than one atom is straightforward [1,6].

The numerical method used to solve the master equations is that of Savage and Carmichael [10,11]. Specifically, the laser master equation (4) can be written as a system of first order, ordinary differential equations

$$\frac{d\rho}{dt}=\hat{\mathbf{L}}\rho \ , \tag{5}$$

using the truncated basis set of number-atom states $\{|n,\beta\rangle, n=0,1,\ldots,N-1;\ \beta=1,2,\ldots,\mu\}$, where n (β) denotes the number (atomic) state. $\hat{\mathbf{L}}$ is a sparse coefficient matrix, and ρ is regarded as a vector of $(N_a\times N)(N_a\times N+1)/2$ elements. With $N=40$ and a four-level atom, $\hat{\mathbf{L}}$ has about 128 800 nonzero elements. For a two-atom laser, the truncated basis set is $\{|n,\beta_1,\beta_2\rangle, n\in\{0,1,\ldots,N-1\};\beta_1,\beta_2\in\{1,2,\ldots,\mu\}\}$, and $\hat{\mathbf{L}}$ has about 3.7×10^6 nonzero elements when $N=40$. The differential equations (5) are solved using the one-step Euler method

$$\rho(t)=\left[\mathbf{I}+\left[\frac{t}{k}\right]\mathbf{L}\right]^k\rho(0) \ , \quad k\to\infty \ . \tag{6}$$

We now derive semiclassical equations for the one-atom lasers from the master equations. The equation of motion for the expectation value $\langle O\rangle$ of any system operator O follows from the master equation (4)

$$\frac{d}{dt}\langle O\rangle=\frac{1}{i\hbar}\langle[O,H]\rangle+\mathrm{Tr}(OL\rho) \ , \tag{7}$$

where $L\rho$ represents all the dissipative terms on the right-hand side of the master equation (4). The equations for the expectation values of the cavity field amplitude, $\langle a\rangle$, and the atomic operators $\langle\sigma_{ij}^{-}\rangle$ are, for the four-level one-atom laser with coherent pumping,

$$\frac{d}{dt}\langle a\rangle=-\kappa\langle a\rangle+g\langle\sigma_{23}^-\rangle ,$$
$$\frac{d}{dt}\langle\sigma_{12}^-\rangle=E\langle\sigma_{24}^+\rangle+g\langle a^\dagger\sigma_{13}^-\rangle-\frac{\gamma_{12}}{2}\langle\sigma_{12}^-\rangle ,$$
$$\frac{d}{dt}\langle\sigma_{13}^-\rangle=E\langle\sigma_{34}^+\rangle-g\langle a\sigma_{12}^-\rangle-\tfrac{1}{2}(\gamma_{13}+\gamma_{23})\langle\sigma_{13}^-\rangle ,$$
$$\frac{d}{dt}\langle\sigma_{14}^-\rangle=E\langle\sigma_4-\sigma_1\rangle-\tfrac{1}{2}(\gamma_{14}+\gamma_{24}+\gamma_{34})\langle\sigma_{14}^-\rangle ,$$
$$\frac{d}{dt}\langle\sigma_{23}^-\rangle=g\langle a^\dagger\sigma_3-a^\dagger\sigma_2\rangle-\tfrac{1}{2}(\gamma_{12}+\gamma_{13}+\gamma_{23})\langle\sigma_{23}^-\rangle , \tag{8}$$
$$\frac{d}{dt}\langle\sigma_{34}^-\rangle=-E\langle\sigma_{13}^+\rangle-g\langle a^\dagger\sigma_{24}^-\rangle -\tfrac{1}{2}(\gamma_{13}+\gamma_{14}+\gamma_{23}+\gamma_{24}+\gamma_{34})\langle\sigma_{34}^-\rangle ,$$
$$\frac{d}{dt}\langle\sigma_1\rangle=E(\langle\sigma_{14}^-\rangle+\langle\sigma_{14}^+\rangle)+\gamma_{12}\langle\sigma_2\rangle +\gamma_{13}\langle\sigma_3\rangle+\gamma_{14}\langle\sigma_4\rangle ,$$
$$\frac{d}{dt}\langle\sigma_2\rangle=g\langle a^\dagger\sigma_{23}^-+a\sigma_{23}^+\rangle-\gamma_{12}\langle\sigma_2\rangle+\gamma_{23}\langle\sigma_3\rangle +\gamma_{24}\langle\sigma_4\rangle ,$$
$$\frac{d}{dt}\langle\sigma_3\rangle=-g\langle a^\dagger\sigma_{23}^-+a\sigma_{23}^+\rangle-(\gamma_{13}+\gamma_{23})\langle\sigma_3\rangle +\gamma_{34}\langle\sigma_4\rangle ,$$

and for the incoherently pumped three-level one-atom laser,

$$\frac{d}{dt}\langle a\rangle=-\kappa\langle a\rangle+g\langle\sigma_{12}^-\rangle ,$$
$$\frac{d}{dt}\langle\sigma_{12}^-\rangle=-\frac{\Gamma}{2}\langle\sigma_{12}^-\rangle+g\langle a\sigma_2-a\sigma_1\rangle-\frac{\gamma_{12}}{2}\langle\sigma_{12}^-\rangle ,$$
$$\frac{d}{dt}\langle\sigma_{13}^-\rangle=-\frac{\Gamma}{2}\langle\sigma_{13}^-\rangle+g\langle a\sigma_{23}^-\rangle-\tfrac{1}{2}(\gamma_{13}+\gamma_{23})\langle\sigma_{12}^-\rangle ,$$
$$\frac{d}{dt}\langle\sigma_{23}^-\rangle=-g\langle a^\dagger\sigma_{23}^-\rangle-\tfrac{1}{2}(\gamma_{12}+\gamma_{13}+\gamma_{23})\langle\sigma_{23}^-\rangle , \tag{9}$$
$$\frac{d}{dt}\langle\sigma_1\rangle=-\Gamma\langle\sigma_1\rangle+g\langle a^\dagger\sigma_{12}^-+a\sigma_{12}^+\rangle+\gamma_{12}\langle\sigma_2\rangle +\gamma_{13}\langle\sigma_3\rangle ,$$
$$\frac{d}{dt}\langle\sigma_2\rangle=-g\langle a^\dagger\sigma_{12}^-+a\sigma_{12}^+\rangle+\gamma_{23}\langle\sigma_3\rangle-\gamma_{12}\langle\sigma_2\rangle .$$

The expectation value $\langle\sigma_i\rangle=\langle\sigma_{ii}\rangle$, is the probability for the electrons to be in atomic level $|i\rangle$. The semiclassical approximation closes these equations by ignoring the correlations between the atomic and field operators. That is, the expectation values containing atomic and field operators are assumed to factorize in Eqs. (8) and (9), e.g., $\langle a\sigma_{23}^-\rangle=\langle a\rangle\langle\sigma_{23}^-\rangle$. This assumption is expected to be valid when the photon number is large.

III. LASER ACTION

In this section we examine the sense in which one pumped atom in a cavity can be regarded as a laser. If the atom is pumped hard enough and the cavity losses are small enough, the system behaves semiclassically and the usual laser theory applies. However, we are interested in the marginal case that is likely to occur in an experimental realization of a one-atom laser. Then the mean cavity photon number may be quite small and the fluctuations in photon number relatively large. Consequently a quantized treatment of the field is required.

To remain faithful to the acronym "laser," light amplification by stimulated emission of radiation, we define our one-atom device to be a laser if the net stimulated emission rate into the cavity mode is much greater than the spontaneous emission rate. For brevity we use the phrase "net stimulated emission rate" to refer to the difference between the stimulated emission and absorption rates. For a multiatom laser the net stimulated emission rate can be large because many photons build up in the laser cavity. However for a one-atom laser with a small number of photons a strong Jaynes-Cummings coupling between cavity mode and atom will be required.

Semiclassically a laser is said to be at threshold when the pumping rate is just sufficient for photon production to balance the losses. This happens when sufficient population inversion, and consequent net stimulated emission, is achieved. However the one-atom laser is not necessarily semiclassical and specifically quantum-mechanical processes may be occurring. Note that although processes such as stimulated and spontaneous emission and absorption may be adequate to describe the physics of semiclassical devices, they may not be sufficient to describe fully quantized systems [12].

We now find expressions for the stimulated and spontaneous emission rates in terms of the diagonal density-matrix elements. For the four-level laser the equations satisfied by the diagonal density-matrix elements for n photons and the lasing levels are, from the master equation (4),

$$\frac{d}{dt}\langle n,2|\rho|n,2\rangle=2\kappa[(n+1)\langle n+1,2|\rho|n+1,2\rangle-n\langle n,2|\rho|n,2\rangle]+g\sqrt{n}\,(\langle n-1,3|\rho|n,2\rangle)+\langle n,2|\rho|n-1,3\rangle) -\gamma_{12}\langle n,2|\rho|n,2\rangle+\gamma_{23}\langle n,3|\rho|n,3\rangle+\gamma_{24}\langle n,4|\rho|n,4\rangle ,$$
$$\frac{d}{dt}\langle n,3|\rho|n,3\rangle=2\kappa[(n+1)\langle n+1,3|\rho|n+1,3\rangle-n\langle n,3|\rho|n,3\rangle]-g\sqrt{n+1}(\langle n+1,2|\rho|n,3\rangle+\langle n,3|\rho|n+1,2\rangle) -\gamma_{13}\langle n,3|\rho|n,3\rangle-\gamma_{23}\langle n,3|\rho|n,3\rangle+\gamma_{34}\langle n,4|\rho|n,4\rangle . \tag{10}$$

For the density-matrix elements determining the coherence between the lasing levels,

$$\frac{d}{dt}\langle n-1,3|\rho|n,2\rangle = 2\kappa[\sqrt{n(n+1)}\langle n,3|\rho|n+1,2\rangle - (n-\tfrac{1}{2})\langle n-1,3|\rho|n,2\rangle] + g(\sqrt{n}\,\langle n-1,3|\rho|n-1,3\rangle - \sqrt{n}\,\langle n,2|\rho|n,2\rangle) - \left[\frac{\gamma_{12}}{2}+\frac{\gamma_{23}}{2}+\frac{\gamma_{13}}{2}\right]\langle n-1,3|\rho|n,2\rangle \ . \tag{11}$$

Now we assume that the first term on the right-hand side, proportional to κ, is small in comparison with the other two terms. We are assuming that $\langle n-1,3|\rho|n,2\rangle \approx \langle n,3|\rho|n+1,2\rangle$, which is reasonable if the photon number distribution is slowly varying, and that the cavity decay rate κ is not too large compared to the coupling g and the atomic decay rates, i.e., the good cavity limit. Assuming a steady state for Eq. (11) and solving for the off-diagonal density-matrix elements, Eqs. (10) become

$$\begin{aligned}\frac{d}{dt}\langle n,2|\rho|n,2\rangle &= 2\kappa[(n+1)\langle n+1,2|\rho|n+1,2\rangle - n\langle n,2|\rho|n,2\rangle] + G_n n(\langle n-1,3|\rho|n-1,3\rangle) - \langle n,2|\rho|n,2\rangle) \\ &\quad -\gamma_{12}\langle n,2|\rho|n,2\rangle + \gamma_{23}\langle n,3|\rho|n,3\rangle + \gamma_{24}\langle n,4|\rho|n,4\rangle \ , \\ \frac{d}{dt}\langle n,3|\rho|n,3\rangle &= 2\kappa[(n+1)\langle n+1,3|\rho|n+1,3\rangle - n\langle n,3|\rho|n,3\rangle] - G_n(n+1)(\langle n,3|\rho|n,3\rangle - \langle n+1,2|\rho|n+1,2\rangle) \\ &\quad -\gamma_{13}\langle n,3|\rho|n,3\rangle - \gamma_{23}\langle n,3|\rho|n,3\rangle + \gamma_{34}\langle n,4|\rho|n,4\rangle \ ,\end{aligned} \tag{12}$$

with

$$\begin{aligned} G_n &= \frac{4g^2}{\gamma_{12}+\gamma_{13}+\gamma_{23}+2\kappa[n-\frac{1}{2}-\sqrt{n(n+1)}]} \\ &\approx \frac{4g^2}{\gamma_{12}+\gamma_{13}+\gamma_{23}} \ , \end{aligned} \tag{13}$$

where the approximate equality follows if the spontaneous emission rates are sufficiently large compared to the cavity damping rate. The terms on the right-hand sides of Eqs. (12) can be identified successively as due to cavity loss, emission into and absorption from the cavity mode, and spontaneous emission into free space. We are thus led to define the excess rate of stimulated emission over absorption to be

$$R_{\rm st} = \sum_{n=0}^{\infty} G_n[n\langle n,3|\rho|n,3\rangle - (n+1)\langle n+1,2|\rho|n+1,2\rangle] \ . \tag{14}$$

Assuming semiclassical factorization of the density matrix, this becomes the semiclassical expression

$$R_{\rm st\ classical} = G_{\langle n\rangle}\langle n\rangle\Delta_{23} \ , \tag{15}$$

where Δ_{23} denotes the population inversion on the lasing levels. The rate of spontaneous emission into the cavity is

$$R_{\rm sp} = \sum_{n=0}^{\infty} G_n\langle n,3|\rho|n,3\rangle \ . \tag{16}$$

Solving the semiclassical version of Eqs. (8) for the coherently pumped four-level laser, we find above threshold,

$$\begin{aligned} \langle n\rangle &= (\gamma_{12}\langle\sigma_2\rangle - \gamma_{23}\langle\sigma_3\rangle)/2\kappa \ , \\ \langle\sigma_2\rangle &= 2E^2[1-(\gamma_{12}+\gamma_{23})\kappa/g^2] \Big/ \left[4E^2 + \frac{\gamma_{12}\gamma_{34}}{2} + \frac{4E^2\gamma_{12}}{\gamma_{34}}\right] \ , \\ \langle\sigma_3\rangle &= \langle\sigma_2\rangle + (\gamma_{12}+\gamma_{23})\frac{\kappa}{2g^2} \ , \end{aligned} \tag{17}$$

where we have assumed that γ_{14} is negligible. The population inversion is then

$$\Delta_{23} = \begin{cases} \kappa(\gamma_{12}+\gamma_{23})/2g^2 & \text{above threshold} \\ <0 & \text{below threshold} \ . \end{cases} \tag{18}$$

For the fully quantum-mechanical case the inversion is obtained by numerically solving the master equation (4) and evaluating

$$\Delta_{23} = \sum_{n=0}^{\infty} (\langle n,3|\rho|n,3\rangle - \langle n,2|\rho|n,2\rangle) \ . \tag{19}$$

Figure 2 presents solutions for the case $g \gg \kappa$, which is not expected to be experimentally feasible. In Fig. 2(a) we plot the mean number of cavity photons versus the coherent pumping field. The semiclassical curve shows a laser threshold where the photon number becomes nonzero. This is a semiclassical signature of laser action. The fully quantum-mechanical result shows that the photon number in the cavity is always nonzero due to spontaneous emission. Far above threshold the semiclassical and quantum-mechanical results agree. The semiclassical laser threshold is at the coherent pumping field $E=0.052$, where semiclassical population inversion first occurs. However in the quantum-mechanical case, population inversion is always present, Fig. 2(b). The solution of the master equation (4) shows that net stimulated emission dominates spontaneous emission well above the semiclassical threshold, Fig. 2(c). This justifies calling the one-atom device a laser.

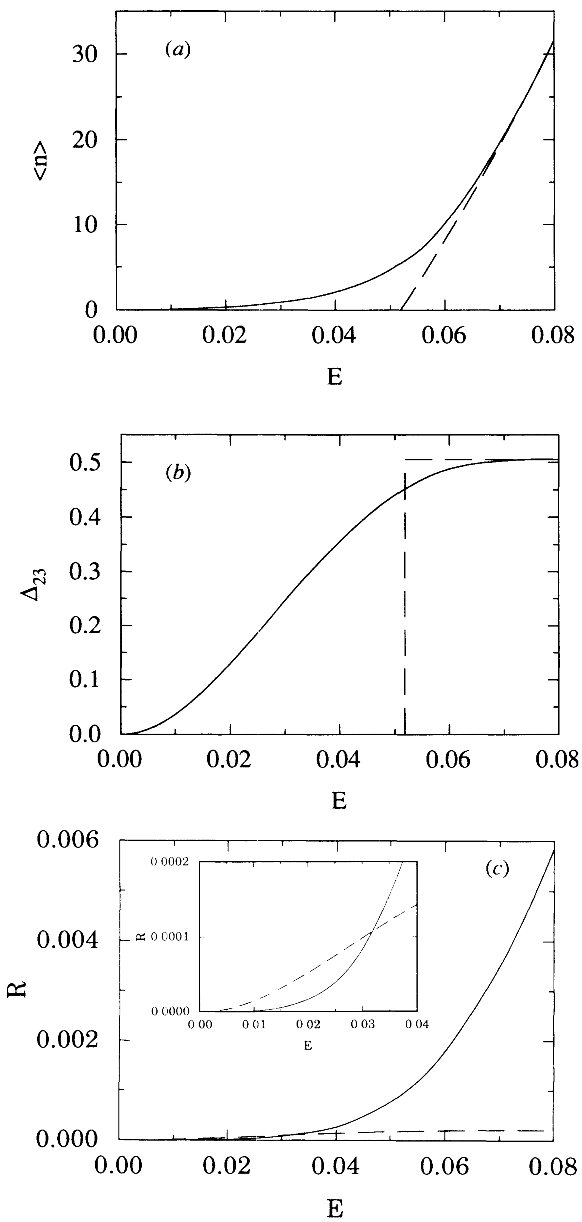

FIG. 2. Evidence for laser action in the coherently pumped four-level one-atom laser. In (a) and (b) the solid curves are obtained from a numerical solution of the master equation (3), and the dashed curves from the semiclassical approximation. (a) The mean number of photons in the cavity vs coherent pumping field E. Semiclassical curve from Eq. (17). (b) Population inversion vs coherent pumping field E, Eq. (19). Semiclassical curve from Eq. (18). (c) Emission rate from lasing levels vs coherent pumping rate, obtained from numerical solution of the master equation (4). The solid curve is the excess rate of stimulated emission over absorption, Eq. (14), and the dashed curve the spontaneous emission rate, Eq. (16). All parameters are scaled by γ_{12} to make them dimensionless and are $\kappa=0.001$, $g=0.01$, $\gamma_{23}=0.01$, $\gamma_{34}=1$, $\gamma_{14}=0$.

In the limit of weak cavity coupling compared to the cavity decay rate, $g \ll \kappa$, it is impossible to achieve lasing for a one-atom laser since the loss rate exceeds that of photon generation. The semiclassical formula for the mean photon number Eq. (17) suggests that to produce laser light, g and κ should be chosen to satisfy the condition

$$\gamma_{12}\langle\sigma_2\rangle-\gamma_{23}\langle\sigma_3\rangle>0 \tag{20}$$

for some pumping rate.

Experimentally it may be possible to achieve an atom-cavity coupling ten times both the cavity and laser transition decay rates $\kappa=\gamma_{23}=0.01\gamma_{12}$, $g=0.1\gamma_{12}$. Figure 3 shows the predicted mean number of cavity photons as a function of the coherent pumping rate. Assuming the atom is at the center of a Gaussian ring cavity mode, the value of the mode function is

$$|u|=(\tfrac{1}{2}\pi L w^2)^{-1/2} , \tag{21}$$

where L is the length of the cavity and w is the mode waist, and the Jaynes-Cummings coupling strength Eq. (2) becomes

$$g=\left[\frac{3\gamma_L c}{4\pi^2 L(w/\lambda)^2}\right]^{1/2} . \tag{22}$$

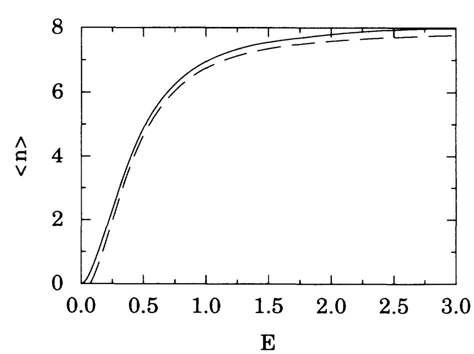

FIG. 3. The mean cavity photon number vs coherent pumping field E for the four-level coherently pumped one-atom laser when κ is larger, and hence more realistic, than in Fig. 2. The solid curve is obtained by numerically solving the master equation (4), and the dashed curve from the semiclassical approximation, Eq. (17). The parameters are again scaled by γ_{12}: $\kappa=0.01$, $g=0.1$, $\gamma_{23}=0.01$, $\gamma_{34}=2$, $\gamma_{14}=0$.

If $\gamma_{12}=10^8 s^{-1}$, so $\gamma_L(=\gamma_{23})=\kappa=10^6 s^{-1}$ and $g=10^7 s^{-1}$, the required cavity finesse $F=\pi c/2L\kappa$ and mode waist are related to the cavity length L in meters by

$$F\approx\frac{500}{L}\ ,\quad \frac{w}{\lambda}\approx\frac{1}{2\sqrt{L}}\ . \tag{23}$$

So for a cavity length of 1 cm the required finesse is $F\approx 50\,000$ and the required mode waist about five wavelengths. Similar conditions have been attained in the laboratory [2]. For a pumping rate in the saturated regime $E=2$ the net stimulated emission rate is seven times greater than the spontaneous emission rate, suggesting laser action is occurring. This can be confirmed by examining the Q-function quasiprobability distribution for the field, Fig. 4. The Q function $Q(\alpha)=\langle\alpha|\rho|\alpha\rangle$ is defined to be the coherent-state diagonal density-matrix elements. It gives a complete description of the quantum-mechanical field. It may be interpreted as the joint probability distribution for measurement of the quadrature phase amplitudes. $Q(\alpha)$ at the phase plane point α is proportional to the probability density for obtaining the real and imaginary parts of α, respectively. The Q function shown in Fig. 4 is typical of a laser. It is centered on zero amplitude and phase symmetric because of laser phase diffusion.

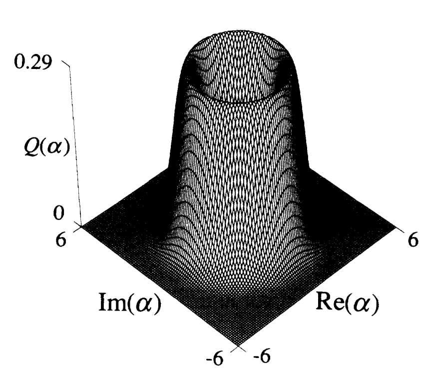

FIG. 4. Q function for the coherently pumped four-level one-atom laser far above threshold, $E=1.5$. Same parameters as Fig. 3.

We now analyze the three-level laser model, Fig. 1(b), in a similar manner. Assuming $g,\gamma_{12}\gg\kappa$, we find, from the master equation (4),

$$\begin{aligned}\frac{d}{dt}\langle n,1|\rho|n,1\rangle &= 2\kappa[(n+1)\langle n+1,1|\rho|n+1,1\rangle - n\langle n,1|\rho|n,1\rangle] + G_n' n(\langle n-1,2|\rho|n-1,2\rangle - \langle n,1|\rho|n,1\rangle)\\ &\quad +\gamma_{12}\langle n,2|\rho|n,2\rangle + \gamma_{13}\langle n,3|\rho|n,3\rangle - \Gamma\langle n,1|\rho|n,1\rangle\ ,\\ \frac{d}{dt}\langle n,2|\rho|n,2\rangle &= 2\kappa[(n+1)\langle n+1,2|\rho|n+1,2\rangle - n\langle n,2|\rho|n,2\rangle] - G_n'(n+1)(\langle n,2|\rho|n,2\rangle - \langle n+1,1|\rho|n+1,1\rangle)\\ &\quad -\gamma_{12}\langle n,2|\rho|n,2\rangle + \gamma_{23}\langle n,3|\rho|n,3\rangle\ ,\end{aligned} \tag{24}$$

with

$$G_n'=\frac{4g^2}{\gamma_{12}+\Gamma+2\kappa(n-\frac{1}{2}-\sqrt{n(n+1)})}\approx\frac{4g^2}{\gamma_{12}+\Gamma}\ . \tag{25}$$

Analogously with Eq. (14) we define the excess rate of stimulated emission over absorption to be

$$R_{\rm st}'=\sum_{n=0}^{\infty}G_n'(n\langle n,2|\rho|n,2\rangle-(n+1)\langle n+1,1|\rho|n+1,1\rangle)\ . \tag{26}$$

In the semiclassical approximation this becomes

$$R_{\rm st\ classical}'=G_{\langle n\rangle}'\langle n\rangle\Delta_{12}\ , \tag{27}$$

where Δ_{12} denotes the population inversion on the lasing levels. The spontaneous emission rate is defined to be

$$R_{\rm sp}'=\sum_{n=0}^{\infty}G_n'\langle n,2|\rho|n,2\rangle\ . \tag{28}$$

Solving the semiclassical version of Eqs. (9), the semiclassical mean photon number above threshold is

$$\begin{aligned}\langle n\rangle &= \frac{\gamma_{23}\Gamma}{2\kappa B}\left\{1-\frac{[\gamma_{23}\Gamma+\gamma_{12}B][\gamma_{13}+\gamma_{23}+\frac{\kappa}{2g^2}(\gamma_{12}+\Gamma)B]}{\gamma_{23}[2(\gamma_{13}+\gamma_{23})+\Gamma]\Gamma}\right\}\ ,\\ B &= \gamma_{13}+\gamma_{23}+\Gamma\ ,\end{aligned} \tag{29}$$

and the semiclassical population inversion is

$$\Delta_{12\,\text{classical}}=\begin{cases}\kappa(\Gamma+\gamma_{12})/2g^2 & \text{above threshold}\\ \dfrac{\gamma_{23}(\Gamma-\gamma_{12})}{\gamma_{12}\gamma_{23}+\Gamma(\gamma_{12}+\gamma_{23})}-\dfrac{1}{\Gamma} & \text{below threshold}\ .\end{cases} \tag{30}$$

For the fully quantum case, the inversion is given by

$$\Delta_{12}=\sum_{n=0}^{\infty}(\langle n,2|\rho|n,2\rangle-\langle n,1|\rho|n,1\rangle)\ . \tag{31}$$

Figure 5 gives the results of solving Eq. (4) numerically, with $g=1$ and $\kappa=0.01$ (all the parameters are also scaled by γ_{12} for this model). According to Fig. 5(a) the full quantum-mechanical solution for the mean photon number versus pumping rate lacks a clear laser threshold. However Fig. 5(c) shows that stimulated emission dominates spontaneous emission into the cavity for a wide range of pumping rates. Hence despite the presence of only 10 to 20 photons in the cavity, it is reasonable to call this device a laser.

IV. ONE-ATOM SUB-POISSONIAN LASER

In this section we consider laser physics, which is not specific to one-atom lasers. However it is useful to study laser properties with the fully quantized one-atom model because unlike other models, no approximations are required for its solution.

Recently it has been predicted that sub-Poissonian, also called intensity squeezed, light can be generated by conventional multilevel lasers [5–8]. This is different from the regular pumping mechanism for reducing population fluctuations [13], which has been successfully realized using diode lasers pumped with sub-shot-noise current [14]. The basic requirement for obtaining sub-Poissonian light without regular pumping is that pumping from the lower lasing level to the upper lasing level have at least two steps with approximately equal transition rates. Hence at least a three-level laser is needed to produce sub-Poissonian light.

The deviation of the photon statistics from Poissonian is quantified by the ratio of the variance to the mean, called the Fano factor

$$F=\frac{\langle n^2\rangle-\langle n\rangle^2}{\langle n\rangle}\ . \tag{32}$$

With a vacuum field outside the cavity the intensity squeezing spectrum outside the cavity is [15]

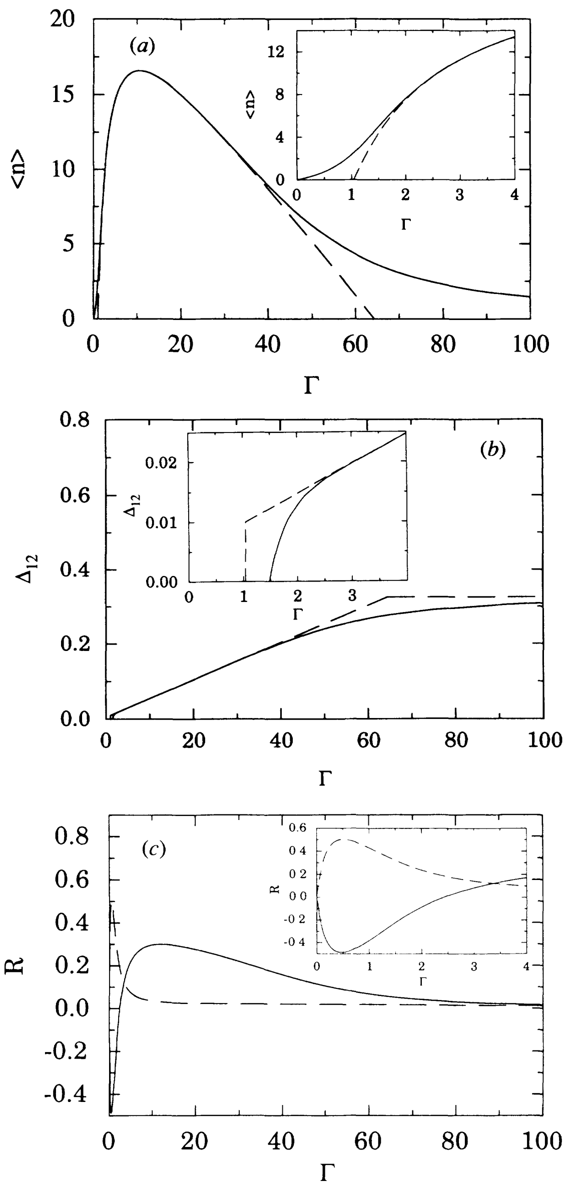

FIG. 5. Evidence for laser action in the incoherently pumped three-level one-atom laser. In (a) and (b) the solid curves are obtained from a numerical solution of the master equation (4), and the dashed curves from the semiclassical approximation. (a) The mean number of photons in the cavity vs incoherent pumping rate Γ. Semiclassical curve from Eq. (29). Note the self-quenching for high pumping rates, discussed in Sec. V. (b) Population inversion vs incoherent pumping rate Γ, Eq. (31). Semiclassical curve from Eq. (30). (c) Emission rate from lasing levels vs incoherent pumping rate, obtained from numerical solution of the master equation (4). The solid curve is the excess rate of stimulated emission over absorption, Eq. (26), and the dashed curve the spontaneous emission rate, Eq. (28). All parameters are scaled by γ_{12} to make them dimensionless and are $\kappa=0.01$, $g=1$, $\gamma_{23}=0.5$, $\gamma_{13}=0$.

$$S(\omega)=1+4\kappa\left\{\mathrm{Re}\left[\int_0^\infty d\tau \exp(i\omega\tau)(g^{(2)}(\tau)-\langle n\rangle^2)\right]\right\}\Big/\langle n\rangle \ , \tag{33}$$

ω is the spectral frequency and the second-order correlation function is defined to be

$$g^{(2)}(\tau)=\lim_{t\to\infty}\langle a^\dagger(t)a^\dagger(t+\tau)a(t+\tau)a(t)\rangle \ . \tag{34}$$

$S(\omega)$ equal to zero corresponds to perfectly regular photon arrivals (c.f. number state) and $S(\omega)$ equal to 1 corresponds to Poissonian photon arrivals (c.f. coherent state). $S(\omega)$ between zero and 1 is referred to as sub-Poissonian statistics. We find $g^{(2)}(\tau)$ using the formula [16]

$$g^{(2)}(\tau)=\mathrm{Tr}\{a^\dagger a \exp(\hat{\mathbf{L}}\tau)[a\rho_s a^\dagger]\} \ , \tag{35}$$

which is valid for Markovian systems. The density operator ρ_s is the stationary solution of the master equation Eq. (4).

In the following we only present results for the coherently pumped four-level laser. The incoherently pumped three- and four-level lasers behave similarly. An intensity squeezing spectrum for the four-level coherently pumped one-atom laser is shown in Fig. 6. The Fano factor for the field outside the cavity, which is the zero-frequency intensity squeezing, can be obtained from the Fano factor inside the cavity via the Mandel Q parameter $Q=F-1$. For the case of Fig. 6 the Q parameters inside and outside the cavity are, respectively, -0.34 and -0.704. So the ratio of the Q parameter outside the cavity to that inside the cavity is about 2.07. This is to be compared with the ratio of 2 predicted if the intensity squeezing spectrum is Lorentzian [7]. We have confirmed by direct calculation of the zero-frequency intensity squeezing that the Q parameter outside the cavity is always a factor of 2.07 greater than that of the light inside cavity for the parameter ranges we consider.

Figure 7 plots the Fano factor of the output field as a function of the coherent pumping field for different atom-cavity coupling strengths. When g is small, $g=0.1$, super-Poissonian light is produced, with only a small amount of squeezing for slow pumping rates. This implies that noise from the lasing transition, from level $|3\rangle$ to level $|2\rangle$, has destroyed the sub-Poissonian statistics. Making g larger, $g=1$, strongly sub-Poissonian light can be produced. In this case the Fano factor agrees well with that predicted by the simple statistical theory of squeezed lasers [6–8]. Since this approach also works well for multiatom lasers, we conclude that provide the atom-cavity coupling is sufficiently large, the physics of squeezed one-atom lasers is the same as that of squeezed multiatom lasers. However if g is not large, a multiatom laser will give better squeezing, since increasing the number of atoms has a similar effect to making the atom-cavity coupling stronger. This suggests that the sub-Poissonian light from a two-atom laser will be better than that from a one-atom laser if g is small enough to make the noise from the lasing transition significant.

To confirm this point we solve the coherently pumped two-atom four-level laser with the same parameters except for smaller g, $g=0.5$. Since the calculation is computationally expensive for two atoms, we only solve for a few coherent pumping fields, namely $E=0.2$, 0.3, 0.4, 0.5. The Fano factors are found to be $F=0.641$, 0.436, 0.331, 0.301 in comparison with the corresponding one-atom laser results $F=0.645$, 0.442, 0.336, 0.305. The light from the two-atom laser is slightly more sub-Poissonian because the effective atom-cavity coupling constant is increased by the square root of the number of atoms, i.e., $\sqrt{2}$.

We now show that the spectral linewidth of a sub-Poissonian laser behaves quite differently to that of a normal laser. A simple expression for the linewidth of a normal laser is due to Schawlow and Townes [17,18]

$$\Delta\omega=\kappa/\langle n\rangle \ . \tag{36}$$

A more exact formula for the normal laser linewidth

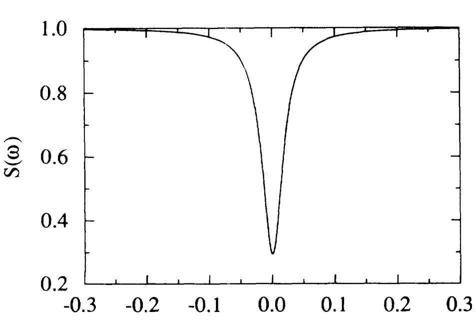

FIG. 6. Intensity squeezing spectrum outside the cavity for a coherently pumped four-level one-atom laser, Eq. (33). ω is scaled by γ_{12} and hence dimensionless. Parameters are the same as Fig. 3, except for $g=1$ and $E=0.5$.

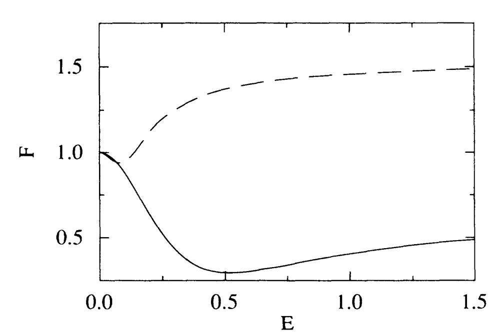

FIG. 7. Fano factor of the laser output field vs coherent pumping field for the four-level one-atom laser. Solid curve is for $g=1$; dashed curve for $g=0.1$. The prediction of the statistical model of Refs. [6–8] (not shown) for $g=1$, agrees very well with the numerically computed curve. Other parameters are the same as for Fig. 3.

above threshold is given by Haken [1]

$$\Delta\omega=\frac{g^2\gamma_{23}}{4\langle n\rangle(\kappa+\gamma_{23})^2}\sum_{n=0}^{\infty}(\langle n,2|\rho|n,2\rangle+\langle n,3|\rho|n,3\rangle)\ . \tag{37}$$

This formula was obtained by treating the lasing levels as a two-level laser and by assuming $g \gg \kappa,\gamma_{23}$. A characteristic feature of these formulas is that the laser linewidth decreases with increasing laser power, i.e., with $\langle n\rangle$. The laser linewidth can be understood as due to phase fluctuations caused by spontaneous emission into the laser mode [18].

The laser spectrum outside the cavity is

$$S(\omega)=A\lim_{t\to\infty}\left\{\mathrm{Re}\int_0^{\infty}\exp(-i\omega\tau)\langle a^{\dagger}(t)a(t+\tau)\rangle d\tau\right\}\ , \tag{38}$$

where A is a normalization constant, and ω is the spectral frequency in radians per second. The first-order correlation function $\langle a^{\dagger}(t)a(t+\tau)\rangle$ is calculated using [16]

$$\langle a^{\dagger}(t)a(t+\tau)\rangle=\mathrm{Tr}\{a(t)e^{\hat{L}\tau}[\rho(t)a^{\dagger}(t)]\}\ , \tag{39}$$

which is valid for Markovian systems. In the limit $t\to\infty$, $\rho(t)$ is the stationary solution of Eq. (4), ρ_s.

The linewidth of the coherently pumped four-level laser is shown as a function of coherent pumping rate in Fig. 8, which should be compared with the corresponding Fano factor graph, Fig. 7. For a cavity field coupling of $g=0.1$ the laser output is super-Poissonian and the laser linewidth increases with pumping rate. This conventional behavior is not followed when g is increased to $g=1$, so that the laser output becomes sub-Poissonian. In this case the laser linewidth increases with pumping rate. Presumably, decreased photon number fluctuations are associated with increased phase fluctuations, giving an increased phase diffusion rate and consequent increased linewidth. Note however that the linewidth does not decrease after the squeezing starts to degrade, above

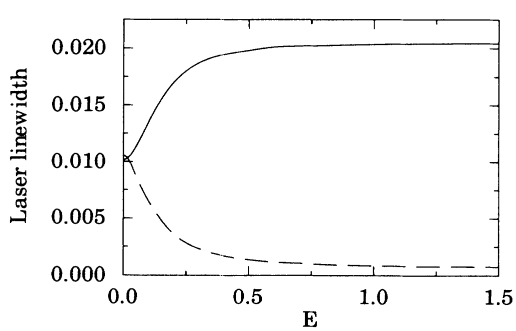

FIG. 8. Linewidth of the four-level laser vs coherent pumping field, from Eq. (38), for the same cases as Fig. 7. The solid curve is for $g=1$, corresponding to sub-Poissonian statistics; the dashed curve is for $g=0.1$, corresponding to super-Poissonian statistics.

$E=0.5$. This is because other factors, such as the electron populations, must also be considered, Eq. (37).

V. SELF-QUENCHING LASERS

In Sec. III we found that for sufficiently high pumping rates the laser power was a decreasing function of the incoherent pumping rate, Fig. 5(a). We refer to this effect as self-quenching. In this section we use semiclassical arguments to show that self-quenching is to be expected in all lasers that are incoherently pumped out the lower laser level. The reason is that the incoherent pumping destroys the coherence between the laser levels, inhibiting the transition. Self-quenching is likely to be particularly significant for one-atom lasers because they must be pumped hard to produce a significant amount of light.

First we show that the effect occurs in the two-level laser in the semiclassical approximation. As described in Sec. II the following semiclassical equations can be derived from the master equation (4) for the two-level laser

$$\begin{aligned}
&\frac{d}{dt}\langle a\rangle=-\kappa\langle a\rangle+g\langle\sigma_{12}^-\rangle\ .\\
&\frac{d}{dt}\langle\sigma_{12}^-\rangle=-\tfrac{1}{2}(\gamma_{12}+\Gamma)\langle\sigma_{12}^-\rangle+g\langle a\rangle\langle\sigma_z\rangle\ ,\\
&\frac{d}{dt}\langle\sigma_z\rangle=-(\gamma_{12}+\Gamma)\langle\sigma_z\rangle-\gamma_{12}+\Gamma-4g\langle a\rangle\langle\sigma_{12}^-\rangle\ ,
\end{aligned} \tag{40}$$

where $\langle\sigma_z\rangle=\langle\sigma_2\rangle-\langle\sigma_1\rangle$. Other variables and parameters are the same as those in Sec. II. For the multiatom laser we adopt the following standard scaling of the variables [1]

$$\langle a\rangle=\sqrt{N_a}\langle\tilde{a}\rangle\ ,\ \langle\sigma_{12}\rangle=N_a\langle\tilde{\sigma}_{12}\rangle\ ,\quad \langle\sigma_z\rangle=N_a\langle\tilde{\sigma}_z\rangle\ , \tag{41}$$

where N_a denotes the number of atoms. The multiatom semiclassical laser equations are then

$$\begin{aligned}
&\frac{d}{dt}\langle\tilde{a}\rangle=-\kappa\langle\tilde{a}\rangle+\sqrt{N_a}g\langle\tilde{\sigma}_{12}^-\rangle\ ,\\
&\frac{d}{dt}\langle\tilde{\sigma}_{12}^-\rangle=-\tfrac{1}{2}(\gamma_{12}+\Gamma)\langle\tilde{\sigma}_{12}^-\rangle+\sqrt{N_a}g\langle\tilde{a}\rangle\langle\tilde{\sigma}_z\rangle\ ,\\
&\frac{d}{dt}\langle\tilde{\sigma}_z\rangle=-(\gamma_{12}+\Gamma)\langle\tilde{\sigma}_z\rangle-\gamma_{12}\\
&\qquad\qquad+\Gamma-4\sqrt{N_a}g\langle\tilde{a}\rangle\langle\tilde{\sigma}_{12}^-\rangle\ .
\end{aligned} \tag{42}$$

Setting the derivatives to zero we find the steady-state solution for the mean photon number above threshold

$$\langle n\rangle=\frac{N_a}{4\kappa}\left[\Gamma-\gamma_{12}-\frac{\kappa}{2N_ag^2}(\gamma_{12}+\Gamma)^2\right]\ . \tag{43}$$

According to this formula the mean photon number has a quadratic dependence on the pumping rate. The mean photon number is zero for

$$\Gamma_{\langle n\rangle=0}=\frac{N_ag^2}{\kappa}-\gamma_{12}\pm\frac{N_ag^2}{\kappa}\left[1-\frac{4\kappa}{N_ag^2}\gamma_{12}\right]^{1/2}\ . \tag{44}$$

The smaller zero is the laser threshold pumping rate, while the larger zero is the self-quenching pumping rate. The pumping rate at which the photon number starts to decrease with increasing pumping rate is halfway between these two values:

$$\Gamma_{\mathrm{start}}=\frac{N_a g^2}{\kappa}-\gamma_{12}\ . \tag{45}$$

Figure 9 shows the mean cavity photon number as a function of pumping rate for the one-atom, $N_a=1$, two-level laser.

The reason for the self-quenching can be identified in the semiclassical laser equations (40). The equation for the atomic polarization $\langle\sigma_{12}^-\rangle$, has a damping term proportional to the sum of the spontaneous emission and incoherent pumping rates. As the polarization is damped to zero at large pumping rates the source term $g\langle\sigma_{12}^-\rangle$ in the field amplitude equation becomes zero and so the field drops to zero. Since the pumping rate at which self-quenching starts, Eq. (45), increases with the number of atoms in the laser, self-quenching will be enhanced in few atom lasers. Other conditions favoring the occurrence of self-quenching are a large cavity loss rate κ and a small Jaynes-Cummings atom-cavity coupling strength, g.

The three-level laser, unlike the two-level laser, can be realized experimentally. Assuming $\gamma_{13}=0$, the semiclassical version of the three-level laser equations (9) yield the following expression for the semiclassical lasing threshold:

$$\Gamma^{(3)}_{\mathrm{threshold}}=2r^{1/3}\cos(\theta+4\pi/3)-u/3\ , \tag{46}$$

where

$$\begin{aligned} r&=\{-[\tfrac{1}{3}(v-\tfrac{1}{3}u^2)]^3\}^{1/2}\ ,\\ \theta&=\tfrac{1}{3}\arccos\left[-\frac{1}{2r}\left[\frac{2}{27}u^3-\tfrac{1}{3}uv+w\right]\right]\ ,\\ u&=\gamma_{12}+\gamma_{23}+\gamma_{23}\left[\gamma_{12}-\frac{2g^2}{\kappa}\right]\bigg/(\gamma_{12}+\gamma_{23})\ ,\\ v&=2\gamma_{12}\gamma_{23}-\frac{2\gamma_{23}(\gamma_{23}-\gamma_{12})g^2}{\kappa(\gamma_{12}+\gamma_{23})}\ ,\\ w&=\gamma_{12}\gamma_{23}^2\left[\gamma_{12}+\frac{2g^2}{\kappa}\right]\bigg/(\gamma_{12}+\gamma_{23})\ . \end{aligned} \tag{47}$$

The pumping rate at which the laser turns completely off is

$$\Gamma^{(3)}_{\mathrm{off}}=2r^{1/3}\cos(\theta)-u/3\ , \tag{48}$$

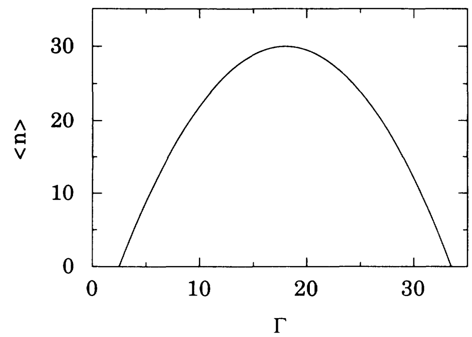

FIG. 9. Cavity photon number vs incoherent pumping rate for the two-level, one-atom laser under the semiclassical approximation, Eq. (43). Parameters are $g=1$, $\kappa=0.05$, $\gamma_{12}=2$.

provided this is greater than the laser threshold Eq. (46). The laser photon number starts decreasing as the pumping rate is increased above the pumping rate,

$$\begin{aligned} \Gamma^{(3)}_{\mathrm{start}}&=2R^{1/3}\cos\left[\frac{1}{3}\arccos\left[-\frac{q}{2R}\right]\right]-\tfrac{5}{3}\gamma_{23}\ ,\\ R&=\left[-\left[\frac{p}{3}\right]^3\right]^{1/2}\ ,\\ p&=-\tfrac{13}{3}\gamma_{23}^2-\frac{4g^2\gamma_{23}}{\kappa}\ ,\\ q&=\tfrac{70}{27}\gamma_{23}^3+\frac{8g^2\gamma_{23}^2}{3\kappa}\ , \end{aligned} \tag{49}$$

where γ_{13} and γ_{12} have been set equal to zero. The laser self-quenching can also be seen in the expression for the excess of stimulated emission over absorption, Eq. (26), since the coefficient G_n', Eq. (25), decreases with increasing pumping rate.

In summary, we have demonstrated that it may be possible to build a one-atom laser. Furthermore we have shown that the fully quantized one-atom model can be solved numerically and exactly in a variety of interesting circumstances. Finally, we examined the phenomenon of self-quenching in incoherently pumped lasers.

ACKNOWLEDGMENT

We acknowledge discussions with Tim Ralph. This work was supported by the Australian Research Council.

[1] H. Haken, in *Light and Matter*, edited by L. Genzel, Handbuch der Physik Vol. XXV/2c (Springer-Verlag, Berlin, 1970).

[2] G. Rempe, R. J. Thompson, R. J. Brecha, W. D. Lee, and H. J. Kimble, Phys. Rev. Lett. **67**, 1727 (1991).

[3] A. M. Smith and C. W. Gardiner, Phys. Rev. A **38**, 4073 (1988).

[4] A. M. Smith and C. W. Gardiner, Phys. Rev. A **41**, 2730 (1990).

[5] A. M. Khazanov, G. A. Koganov, and E. P. Gordov, Phys. Rev. A **42**, 3065 (1990).

[6] T. C. Ralph and C. M. Savage, Opt. Lett. **16**, 1113 (1991); Phys. Rev. A **44**, 7809 (1991).

[7] H. Ritsch, P. Zoller, C. W. Gardiner, and D. F. Walls,

Phys. Rev. A **44**, 3361 (1991).
[8] H. Ritsch and P. Zoller, Phys. Rev. A **45**, 1881 (1992).
[9] W. H. Louisell, *Quantum Statistical Properties of Radiation* (Wiley, New York, 1973).
[10] C. M. Savage and H. J. Carmichael, IEEE J. Quantum Electron. **24**, 1495 (1988).
[11] C. M. Savage, J. Mod. Opt. **37**, 1711 (1990).
[12] C. M. Savage, Phys. Rev. Lett. **60**, 1828 (1989).
[13] Y. M. Golubev and I. V. Sokolov, Zh. Eksp. Teor. Fiz. **87**, 408 (1984) [Sov. Phys.—JETP **60**, 234 (1984)].
[14] Y. Yamamoto, S. Machida, and O. Nilsson, Phys. Rev. A **34**, 4025 (1986).
[15] H. Ritsch, Quantum Opt. **2**, 189 (1990).
[16] C. W. Gardiner, *Handbook of Stochastic Methods,* 2nd ed. (Springer, Berlin, 1985).
[17] A. L. Schawlow and C. H. Townes, Phys. Rev. **112**, 1940 (1958).
[18] R. Loudon, *The Quantum Theory of Light* (Clarendon, Oxford, 1973).

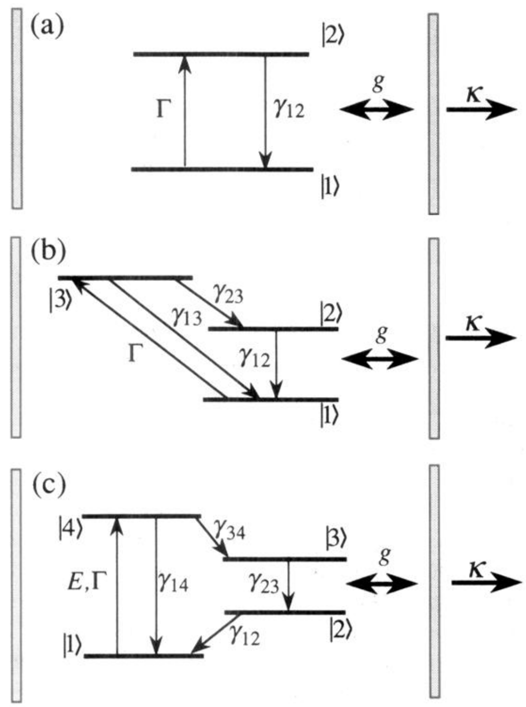

FIG. 1. Schematic diagrams of the laser systems considered in this paper. Pumping is either incoherent at rate Γ or coherent with field strength proportional to E. The arrow labels correspond to terms in the master equation (4). The shaded vertical bars represent cavity mirrors. (a) Two-level laser; (b) three-level laser; (c) four-level laser.

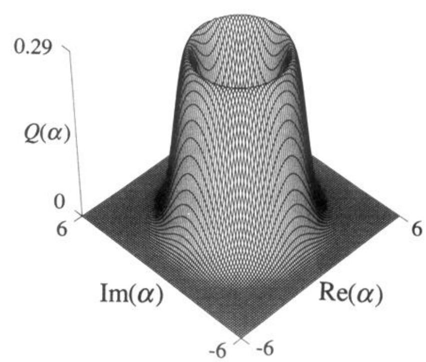

FIG. 4. Q function for the coherently pumped four-level one-atom laser far above threshold, $E = 1.5$. Same parameters as Fig. 3.